Behavior of Railway Cars in Running (Report 4)
—— Basic Consideration on Rail Deformation ——

Seinosuke ARAI

Abstract

The deformation of rail or wheel in the lateral direction in view from large scale is considered to make little influence to the stability or the derailment of a railway car in running. This report aims to clear the extent of its influence and begins with basic problems. They are friction variation with spin motion and deflection of rail.

1. General

In the preceeding reports the auther described about the running stability and the safety of railway cars especially on their derailment phenomena. In connection with running stability or derailment of railway cars, the statics between wheel and rail were studied. Wheel-tire and rail were supposed to be rigid except the partial deformation at the surface area of tire-rail contact.

This report describes the fundamental analysis on the deformation of rails provided wheel-tread with various inclination. Rails are simpified to long and thin steel plate with one of the long and parallel edges clamped and the other free. Wheels are also simplified to steel cylinders which edges are cut to form planned cut angles representing wheel franges or wheel-treads.

2. Statics of Cylinder with Taper Edge on Thin Plate

2-1 Setting a taper-edge cylinder on thin parallel plates

Let a taper-edge cylinder and thin plate call wheel and rail respectively. In case that the wheel slides downward to rail, as in Fig. 2.2, equiliblium of forces acting to the wheel in vertical and in lateral leads the following equations;

$$N\cos\alpha+\mu_0 N\sin\alpha-W=0 \quad \cdots\cdots(2.1)$$

$$F_s-N\sin\alpha+\mu_0 N\cos\alpha=0 \quad \cdots\cdots(2.2)$$

where μ_0 represents frictional coefficient of wheel to rail.

In case that no sliding occurs under the wheel-rail friction the following equations hold;

$$N\cos\alpha+\mu N\sin\alpha-W=0 \quad \cdots\cdots(2.3)$$

$$F_s-N\sin\alpha+\mu N\cos\alpha=0 \quad \cdots\cdots(2.4)$$

where $0<\mu\leqq\mu_0$, and then;

Received Oct. 5, 1983

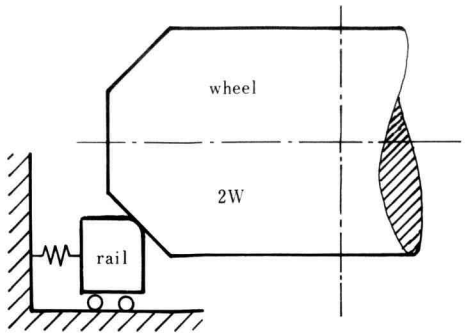

Fig. 2.1 Model of rail and wheel in contact

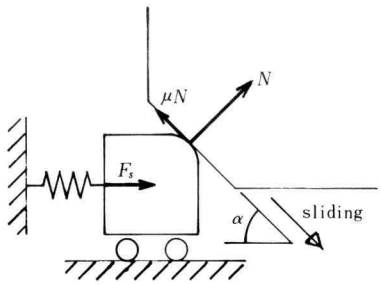

Fig. 2.2 Wheel sliding downward

$$N\cos\alpha+\mu_0 N\sin\alpha-W\geqq 0 \quad \cdots\cdots(2.5)$$

$$F_s-N\sin\alpha+\mu_0 N\cos\alpha\geqq 0 \quad \cdots\cdots(2.6)$$

At the critical condition the above-mentioned eqs. (2.1) and (2.2) hold again.

In the certain range of angle α, the wheel slides downward at first and rail is bent which makes the spring force F_s increase. For small angle α, however, F_s does not increase and it holds zero. To find a critical value of angle α, let $F_s=0$ in the eqs. (2.1) and (2.2);

$$N\cos\alpha_d+\mu_0 N\sin\alpha_d-W=0 \quad \cdots\cdots(2.7)$$

$$N\sin\alpha_d-\mu_0 N\cos\alpha_d=0 \quad \cdots\cdots(2.8)$$

where α_d represents a critical value of α in downward sliding of wheel.
Thus,

$$\tan\alpha_d=\mu_0 \quad \cdots\cdots(2.9)$$

$$N(1+\mu_0^2)=\frac{W}{\cos\alpha_d} \quad \cdots\cdots(2.10)$$

Denoting θ to the frictional angle, then we have;

$$\mu_0=\tan\theta \text{ or } \alpha_d=\theta \quad \cdots\cdots(2.11)$$

$$N(1+\tan^2\theta)=\frac{W}{\cos\theta} \text{ or } N=W\cos\theta \quad \cdots\cdots(2.12)$$

Downward critical angle α, which is α_d, is equal to the frictional angle θ. Note that to fit the above-mentioned analysis the wheel has to be set on the rails almost statical way, that is, no inertia force is produced.

2.2 Releasing the force after pushing the wheel downward

Assuming that the angle α is larger than the critical value α_d in the preceeding section, we can see the forces acting to the wheel are ballanced after sinking with broadening the width between rails.

At the equiliblium condition, if the wheel be loaded by $2\Delta W$, it will sink until the resultant force becomes zero. In a certain range of angle α, the wheel moves upward after removing the load $2\Delta W$ which is sufficiently heavier than the component of frictional force

between rail and wheel on moving upward minus wheel weight.

For the comparatively large angle α, that is $\alpha \geqq \alpha_u$ where α_u represents critical value of α for upward sliding of wheel, the unloaded wheel does not move upward under wedge effect. In this case, the direction of the frictional force is oppsite to that when the wheel slides downward. So in the similar way to downward sliding of wheel;

$$N \cos \alpha_u - \mu_0 N \sin \alpha_u - W \geqq 0 \quad \cdots\cdots (2.13)$$

$$N \sin \alpha_u + \mu_0 N \cos \alpha_u - F_s = 0 \quad \cdots\cdots (2.14)$$

Then

$$\frac{\cos \alpha_u - \mu_0 \sin \alpha_u}{\sin \alpha_u + \mu_0 \cos \alpha_u} \geqq \frac{W}{F_s} \quad \cdots\cdots (2.15)$$

Substituting $\alpha_u = \frac{\pi}{2} - \beta$,

$$\frac{\sin \beta - \mu_0 \cos \beta}{\cos \beta + \mu_0 \sin \beta} \geqq \frac{W}{F_s} \quad \cdots\cdots (2.16)$$

$$\tan (\beta - \theta) \geqq \frac{W}{F_s} \quad \cdots\cdots (2.17)$$

At the critical, that is $F_s = \infty$,

$$\tan (\beta - \theta) = 0, \quad \beta = \theta \text{ or } \alpha_u = \frac{\pi}{2} - \theta \quad \cdots\cdots (2.18)$$

As remarks of this chapter, by denoting θ to frictional angle,

(1) $\alpha \leqq \theta$: Rail is not deflected.

(2) $\alpha \geqq \frac{\pi}{2} - \theta$: Wheel is fixed after removing heavy load due to the principle of wedge effect.

(3) $\theta < \alpha < \frac{\pi}{2} - \theta$: Rail is deflected by the wheel weight plus or minus the vertical component of frictional force.

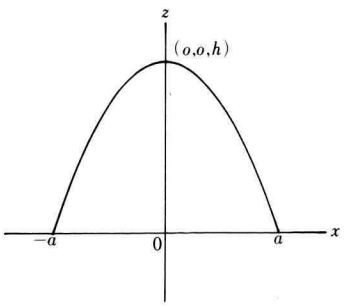

Fig. 3.1 Deflection distribution on z-x plane

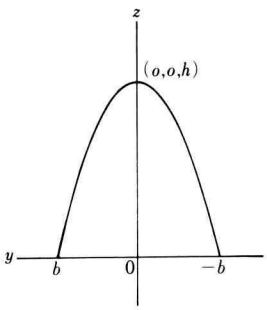

Fig. 3.2 Deflection distribution on y-z plane

3. Apparent Frictional Coefficient When Spin Motion Exists

3.1 Pressure distribution over the surface of contact area

The contact surfaces between wheel-tread and rail take the shape of ellipse[4] with a and b being long and short semiaxes respectively.

Let denote h to the maximum deflection as shown in Fig. 3.1 or Fig. 3.2, where coordinates are oriented as in these figures. Assuming that the deflection be expressed as the followings;

$$z=h-\frac{h}{b^2}y^2 \quad \text{at } x=0 \qquad \cdots\cdots(3.1)$$

$$z=h-\frac{h}{a^2}x^2 \quad \text{at } y=0 \qquad \cdots\cdots(3.2)$$

and also

$$z=h-\frac{h}{a^2}x^2-\frac{h}{b^2}y^2 \qquad \cdots\cdots(3.3)$$

Using these expressions, we again assume the force function like;

$$f(x,\ y)=kz \qquad \cdots\cdots(3.4)$$

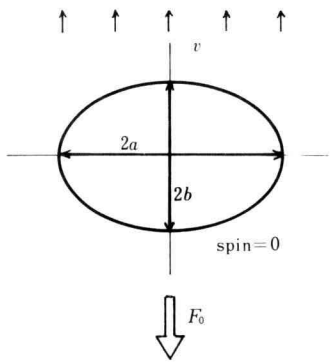

Fig. 3.3 Elliptic surface of contact area

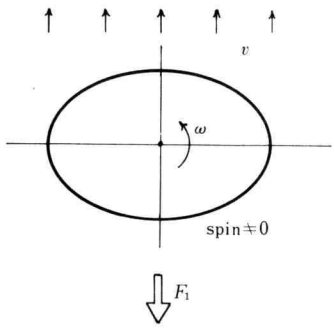

Fig. 3.4 Spin motion added to parallel motion

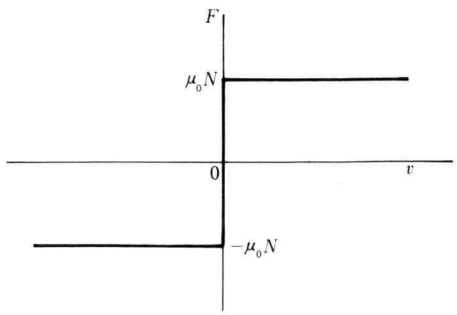

Fig. 3.5 Simplified characteristics of frictional force

Thus

$$N=\int\int f(x,\ y)dxdy \quad \cdots\cdots(3.5)$$

where N represents total pressure or force over the surface of contact area.

3.2 Sliding with spin motion

Figure 3.3 shows an elliptic area of contact zone. v means relative sliding speed between wheel and rail. F_0 means frictional force and is expressed like;

$$F_0=\mu_0 N \quad \cdots\cdots(3.6)$$

and

$$N=\int\int f(x,\ y)dxdy \quad \cdots\cdots(3.7)$$

Figure 3.4 shows that spin motion is overlapped with sliding, where ω represents angular speed of spin. Figure 3.5 is a simplified characteristics of frictional force, which is necessary on the calculation of apparent frictional force including spin motion.

3.3 Execution of integration to obtain the value of k

Substituting (3.4) into (3.5) and using (3.3), we get;

$$N=\int\int k\left(h-\frac{h}{a^2}x^2-\frac{h}{b^2}y^2\right)dxdy=khab\int\int\left(1-\frac{x^2}{a^2}-\frac{y^2}{b^2}\right)d\left(\frac{x}{a}\right)d\left(\frac{y}{b}\right) \qquad (3.8)$$

$$N=khab\int_{-1}^{1}dY\int_{-\sqrt{1-Y^2}}^{\sqrt{1-Y^2}}(1-X^2-Y^2)dX$$

where $X=\frac{x}{a},\ Y=\frac{y}{b}$

$$N=\frac{4}{3}khab\int_{-1}^{1}(1-Y^2)^{\frac{3}{2}}dY=\frac{4}{3}khab\times\frac{3\pi}{8}=\frac{\pi}{2}khab \quad \cdots\cdots(3.9)$$

Thus

$$k=\frac{2}{habn}N \quad \cdots\cdots(3.10)$$

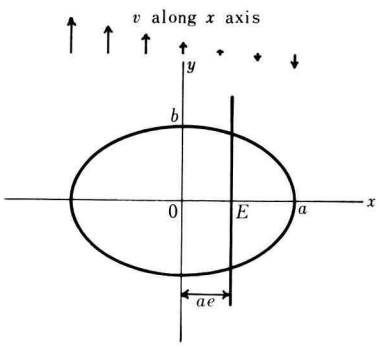

Fig. 3.6 Apparent spin center E

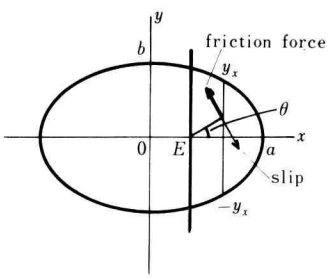

Fig. 3.7 Slip direction of wheel around point E

3.4 Change of frictional force by spin effect

Denoting v_p to the peripheral speed of spin at the point $(a, 0)$, that is the edge of contact elliptic area, v to the speed of parallel motion in the y direction, and r_p to the ratio v/v_p, then r_p is suitable to express the apparent spin center, which is represented by E in Fig. 3.6. $e=0$ at $r_p=0$, and $e=+1$ at $r_p=-1$. It is clear that the following relation holds;

$$e=-r_p \quad \cdots\cdots(3.11)$$

Denoting E in Fig. 3.6 to the apparent spin center, the left side of line $x=ae$ moves upward, whereas the right side moves downward, so that the difference of frictional forces of both sides acts in the y direction. Let the integration of frictional force in the y direction name apparent frictional force, then apparent frictional coefficient is defined by the ratio of apparent frictional force in the y direction to the normal force.

Denoting $\mu_0 F(e)$ to the total frictional force in the y direction, it is expressed as follows;

$$\mu_0 F(e)=-\mu_0 \int_{-a}^{a}\int_{-yx}^{yx}\cos\theta\cdot f(x, y)dxdy, \quad 0<e \quad \cdots\cdots(3.12)$$

where θ is shown in Fig. 3.7.

$$\tan\theta=\frac{y}{x-ae} \quad \cdots\cdots(3.13)$$

then

$$\cos\theta=\frac{x-ae}{\sqrt{y^2+(x-ae)^2}}, \quad -\pi\leqq\theta\leqq\pi \quad \cdots\cdots(3.14)$$

and from the expressions (3.3), (3.4) and (3.10);

$$f(x, y)=\frac{2N}{ab\pi}\left(1-\frac{x^2}{a^2}-\frac{y^2}{b^2}\right) \quad \cdots\cdots(3.15)$$

Substituting (3.14), (3.15) to (3.12), we obtain;

$$\begin{aligned}F(e)&=-\int_{-a}^{a}dx\int_{-yx}^{yx}\frac{x-ae}{\sqrt{y^2+(x-ae)^2}}\cdot\frac{2N}{ab\pi}\left(1-\frac{x^2}{a^2}-\frac{y^2}{b^2}\right)dy\\&=-\frac{2N}{\pi}\int_{-1}^{1}dX\int_{-\sqrt{1-X^2}}^{\sqrt{1-X^2}}\frac{(a/b)(X-e)(1-X^2-Y^2)}{\sqrt{Y^2+(a/b)^2(X-e)^2}}dY\\&=\frac{2N}{\pi}\int_{-1}^{1}I(X, e)\,dX \quad \cdots\cdots(3.16)\end{aligned}$$

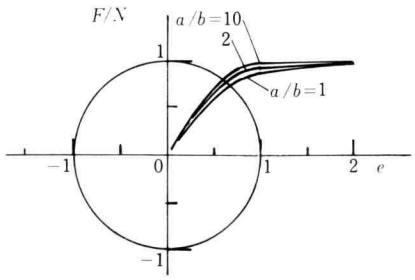

Fig. 3.8 Change of F/N by e

where $X=x/a$, $Y=y/b$ and

$$I(X, e)=-\int_{-\sqrt{1-X^2}}^{\sqrt{1-X^2}} \frac{(a/b)(X-e)(1-X^2-Y^2)}{\sqrt{Y^2+(a/b)^2(X-e)^2}}dY$$

Representing as,

$$(a/b)(X-e)=A_x$$

$$I(X, e)=2A_x\int_0^{\sqrt{1-X^2}} \frac{Y^2+X^2-1}{\sqrt{Y^2+A_x^2}}dY=A_x\sqrt{1-X^2}\sqrt{1-X^2+A_x^2}$$

$$+2A_x(X^2-1-A_x^2/2)\left[\log\{\sqrt{1-X^2}+\sqrt{1+X^2+A_x^2}/\sqrt{A_x^2}\}\right] \cdots\cdots(3.17)$$

$$\mu(e)=\mu_0 F(e)/N=\frac{2\mu_0}{\pi}\int_{-1}^{1} I(X, e)dX \cdots\cdots(3.18)$$

where $\mu(e)$ represents apparent frictional coefficient. Figure 3.8 shows the variation of the value of $F(e)/N$ with e.

4. Deformation of a Rail by an Axial Load of a Wheel[1),2)]

The problem is simplified to that a thin plate cantilever is acted by a concentrated load at the free edge.

Consider a plate in the shape of infinite length with width a and thickness h, which is clamped along one of its parallel edges, the other edge being free. Let the plate be acted by a vertical concentrated load P whose point of application is at the free edge as shown in Fig. 4.1. A Cartesian co-ordinate system $Oxyz$ is introduced, such that the y-axis is in the longitudinal direction, the x-axis is in the direction of width and the z-axis is perpendicular to x-y plane, which are shown in Fig. 4.1.

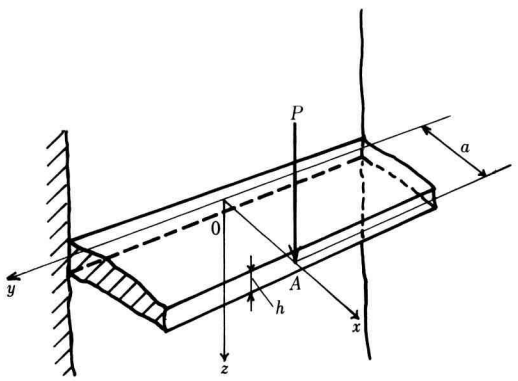

Fig. 4.1 Cantilever plate co-ordinate system and load at point A

Thickness h of the plate is assumed to be far smaller than width a, and the weight of the plate is neglected in the expression. The vertical deflections, which is represented by $\omega(x, y)$, are characterized by a homogeneous biharmonic equation,

$$\nabla^4\omega(x, y)=0 \cdots\cdots(4.1)$$

which is valid throughout the regions under consideration except for a singular point A.

$$\left(\nabla^4=\frac{\partial^4}{\partial x^4}+2\frac{\partial^4}{\partial x^2\partial y^2}+\frac{\partial^4}{\partial y^4}\right)$$

4.1 Applying a vertical concentrated load P at point A

The equation relating the deflections to the shearing forces, bending moments and twisting moments are

$$\left.\begin{aligned} Q_x &= -D(w_{xxx}+w_{xyy}) \\ M_x &= -D(w_{xx}+\nu w_{yy}) \\ M_y &= -D(w_{yy}+\nu w_{xx}) \\ M_{xy} &= -M_{yx}=D(1-\nu)w_{xy} \end{aligned}\right\} \quad \cdots\cdots(4.2)$$

where ν is Poisson's ratio, $D=Eh^3/\{12(1-\nu^2)\}$, E is Young's modulus and the subscripts x and y attached to w indicate partial derivatives. For example;

$$w_{xyy}=\frac{\partial^3 w}{\partial x\partial y^2} \quad \cdots\cdots(4.3)$$

Concerning the equations (4.2), the boundary conditions written in terms of the deflection w, are as follows: Along the clamped edge,

$$\left.\begin{aligned} w(0,\ y)&=0 \\ w_x(0,\ y)&=0 \end{aligned}\right\} \quad \cdots\cdots(4.4)$$

and along the free edge,

$$\left.\begin{aligned} M_x(a,\ y)&=0 \\ Q_x(a,\ y)&=0 \\ M_{xy}(a,\ y)&=0 \end{aligned}\right\} \quad \cdots\cdots(4.5)$$

so that,

$$[w_{xx}+\nu w_{yy}]\ (a,\ y)=0 \quad \cdots\cdots(4.6)$$

$$[w_{xxx}+(2-\nu)w_{xyy}]\ (a,\ y)=0 \quad \cdots\cdots(4.7)$$

where equation (4.7) is equivalent to the requirements $Q_x(a,\ y)=0$ and $M_{xy}(a,\ y)=0$.[3)]

The shearing force Q_x must be continuous along $x=a$, except for the point of application A of the load, where Q_x has discontinuity. The corresponding transition condition is formulated by replacing the concentrated load P with a forcing function $F(y)$ defined by

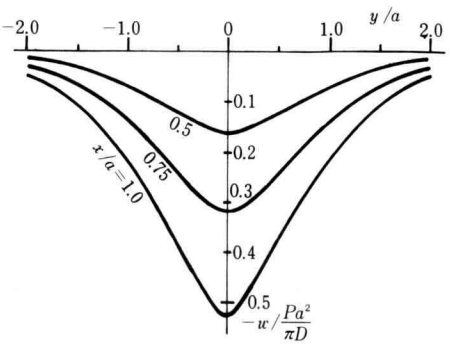

Fig. 4.2 Deflection curves along free edge, x/a=0.75 and 0.5

$$\left.\begin{aligned} F(y)&=p \quad \text{for} \quad |y| \leqq \delta \\ F(y)&=0 \quad \text{for} \quad \delta < |y| \end{aligned}\right\} \cdots\cdots (4.8)$$

where $2p\delta = P$, and by subsequently taking the limit as $\delta \to 0$.

Using the Fourier integral representation for $F(y)$, the required condition on Q_x now becomes,

$$-D[w_{xxx}+w_{xyy}]\ (a,\ y)=\int_0^\infty \frac{2p \sin \alpha\delta}{\pi\alpha} \cos \alpha y d\alpha \quad \cdots\cdots (4.9)$$

4.2 Solution for deflections in integral form

The problem formulated in the preceeding section is to determine the biharmonic function $w(x, y)$, which satisfies the boundary conditions.

To this end it is expressed that,

$$w(x,\ y)=\int_0^\infty f(x,\ \alpha) \cos \alpha y d\alpha \cdots\cdots (4.10)$$

with

$$f(x,\ \alpha)=(A'+B'\alpha x) \cosh \alpha x+(C'+D'\alpha x) \sinh \alpha x \quad \cdots\cdots (4.11)$$

is a solution of equation (4.1) for arbitrary choice of the functions $A'(\alpha)$, $B'(\alpha)$, $C'(\alpha)$, and $D'(\alpha)$.

The deflection curve along the free edge is obtained using partially numerical calculation. Figure 4.2 shows the deflection curve by y/a as the abscissa.

5. Remarks

The quantity of torque with spin motion, its effect to rail deflection and experimental results will be described in the proceeding reports.

References

1) "Deflections and Moments Due to a Concentrated Load on a Cantilever Plate of Infinite Length", by T.J. Jaramillo, Journal of Applied Mechanics, Mar, 1950, p. 67.

2) "Deflection of a Long Helical Gear Tooth", by C.M. MacGregor, Mechanical Engineering, vol. 57, 1935, p. 225.

3) "Theory of Plates and Shells", by S. Timoshenko, McGraw-Hill Book Company, Inc., New York, N.Y., 1940.

4) "Theory of Elasticity", by S.P. Timoshenko and J.N. Goodier, McGraw-Hill, Third Edition, p. 414.